Applied Catalysis B: Environmental 170-171 (2015) 135–143

Contents lists available at ScienceDirect

Applied Catalysis B: Environmental

journal homepage: www.elsevier.com/locate/apcatb

# DFT study on the reaction mechanisms behind the catalytic oxidation of benzyl alcohol into benzaldehyde by $O_2$ over anatase $TiO_2$ surfaces with hydroxyl groups: Role of visible-light irradiation

Hisayoshi Kobayashi [a,*], Shinya Higashimoto [b,**]

[a] Department of Chemistry and Materials Technology, Kyoto Institute of Technology, Matsugasaki, Sakyo-ku, Kyoto 606-8585, Japan
[b] Department of Applied Chemistry, Osaka Institute of Technology, 5-16-1 Omiya, Asahi-ku, Osaka 535-8585, Japan

ARTICLE INFO

*Article history:*
Received 2 December 2014
Received in revised form 22 January 2015
Accepted 25 January 2015
Available online 28 January 2015

*Keywords:*
DFT calculation
Reaction mechanism
$TiO_2$
Selective oxidation of alcohol
Alkoxide

ABSTRACT

Theoretical study on the catalytic oxidation of benzyl alcohol by molecular oxygen ($O_2$) on the $TiO_2$ surface was performed by DFT calculations. The anatase $TiO_2$ crystal faces in the absence and presence of surface hydroxyl groups were modeled with a slab of $Ti_{16}O_{32}$ and $Ti_{16}O_{32}$(OH)H, respectively. The interaction of benzyl alcohol with $Ti_{16}O_{32}$ and $Ti_{16}O_{32}$(OH)H was calculated. It was clearly demonstrated that the surface hydroxyl groups on the $TiO_2$ surface play a significant role in the formation of the alkoxide ([Ti]—O—$CH_2$—ph) species. The orbitals of the alkoxide species was found to be hybridized with the O2p orbital in the valence band (VB) of the $TiO_2$. The origin of the visible-light response in the photocatalytic system can be attributed to the electronic transition from the donor levels created by the alkoxide species to the conduction band (CB). Furthermore, reaction coordinates in the overall catalytic reaction of benzyl alcohol into benzaldehyde on the $TiO_2$ surface were demonstrated, and the role of the visible-light irradiation was also discussed.



## 1. Introduction

The development of organic synthesis for the partial oxidation of alcohols into aldehydes or ketones has been the focus of much attention since such chemical reactions are a fundamental but significant procedure in commercial applications [1–3]. In particular, the use of clean oxidants such as $O_2$ is highly desired over conventional stoichiometric oxidizing agents such as Cr(VI) and peroxy acids.

Organic synthesis by semiconductor photocatalysts is of particular interest since the reaction can proceed by unlimited solar irradiation at room temperature [4–7]. Hence, the selective photocatalytic oxidation of alcohols by $O_2$ under UV-light and/or visible-light irradiation on such photocatalyst as pure $TiO_2$ [8–14], dye-sensitized $TiO_2$ [15], gold nano- particles supported $TiO_2$ or $CeO_2$ [16,17], $Fe^{3+}$ or $Rh^{3+}$ ions modified $TiO_2$ [18,19], nitrogen-doped $TiO_2$ [20], $Nb_2O_5$ [21,22] and carbon nitride ($C_3N_4$) [23] have been widely studied.

In general, anatase $TiO_2$ is known to exhibit photocatalysis only under UV-light irradiation. However, we have previously reported that the photocatalytic oxidation of benzyl alcohol and its derivatives, such as 4-methoxybenzyl alcohol, 4-chlorobenzyl alcohol, 4-nitrobenzyl alcohol, 4-methylbenzyl alcohol, 4-(trifluoromethyl) benzyl alcohol, and 4-tertiary-butylbenzyl alcohol into corresponding aldehydes proceeded at high conversion and selectivity on a $TiO_2$ photocatalyst under $O_2$ atmosphere [11,13]. The reaction was confirmed to proceed under irradiation with both UV-light and visible light. In particular, the visible light response was observed to be attributed to a characteristic surface complex (alkoxide species) formed by the adsorption of a benzyl alcohol on the $TiO_2$ surface. It was confirmed that the charge separation, i.e., holes ($h^+$) and electrons ($e^-$) induced in the alkoxide play a significant role in the selective oxidation of benzyl alcohol by assistance of $O_2$.

A combined experimental and theoretical study of the interaction between the adsorbate and catalyst surface is important in understanding the chemical nature of the surface complex [24,25]. In collaboration with Li et al., the authors have performed a theoretical study via DFT calculations on the interaction of the $TiO_2$ surface with such adsorbate as benzyl alcohol and benzaldehyde [9]. The interaction of benzyl alcohol with the $TiO_2$ surface induced orbital mixing between the anti-bonding $\pi$ molecular orbitals (MO) of a phenyl group and the O2p atomic orbitals (AOs) of $TiO_2$ in

* Corresponding author. Tel.: +81 75 724 7561; fax: +81 75 724 7580.
** Corresponding author. Tel.: +81 6 6954 4283; fax: +81 6 6957 2135.
*E-mail addresses:* hisa@kit.ac.jp (H. Kobayashi), higashimoto@chem.oit.ac.jp (S. Higashimoto).

http://dx.doi.org/10.1016/j.apcatb.2015.01.035
0926-3373/

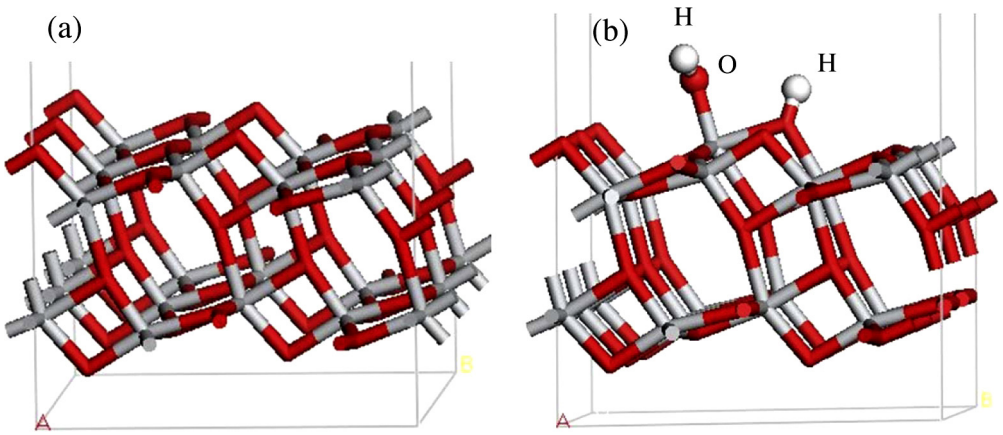


**Fig. 1.** Unit cells models with (a) $Ti_{16}O_{32}$ and (b) $Ti_{16}O_{32}(OH)H$.

the band-gap region, while that of benzaldehyde did not induce orbital mixing. This characteristic feature supports the experimental observation that photo-produced benzaldehyde is not oxidized further to benzoic acid or $CO_2$ [11]. However, they were limited to the interaction of adsorbate with the $TiO_2$ surface.

The purpose of this study is to clarify the overall reaction mechanism for the catalytic oxidation of benzyl alcohol into benzaldehyde by $O_2$ on the $TiO_2$ surface. In this study, reaction coordinates were calculated in the ground states. Therefore, it can be considered that the activation energy which cannot be overcome by thermal energy at 298 K should be afforded by the photo-energy. Here, we have investigated local minima (LMs) and transitional states (TSs) at several reaction paths using the periodic DFT calculations. In particular, we have focused on providing an understanding of: (1) the role of the surface hydroxyl (OH) groups over the $TiO_2$ surface on the catalytic activity; (2) the origin of the visible-light response; and (3) activation mechanisms of the methylene C—H bond.

## 2. Calculation methods

DFT calculations with the periodic boundary conditions were carried out. A plane wave-based program, CASTEP, was employed throughout in the calculations [26,27]. The Perdew–Burke–Ernzerhof (PBE) functionals [28,29] were used together with the ultrasoft-core potentials [30]. The basis set cut-off energies were fixed at 300 eV. The electron configurations of the atoms were Ti: $3s^2 3p^6 4s^2 3d^2$, H: $1s^1$, C: $2s^2 2p^2$, and O: $2s^2 2p^4$. Geometric optimization of all atomic coordinates was carried out within the unit cell, while the lattice constants ($a$ = 7.552 Å, $b$ = 10.210 Å, $c$ = 30 Å, $\alpha$ = 88.99°, and $\beta = \gamma$ = 90°) were fixed. The anatase $TiO_2$ (1 0 1) crystal faces in the absence and presence of surface hydroxyl groups were modeled with a slab of $Ti_{16}O_{32}$ and $Ti_{16}O_{32}(OH)H$, respectively, as shown in Fig. 1. The atoms belonging to the $TiO_2$ lattice are specified in square brackets. The reaction coordinates involving the local minima (LMs) and transitional states (TSs) were identified in the ground states. The stabilization energy ($\Delta E$) was calculated in the following Eq. (1):

$$\Delta E = E(\mathrm{A} \bullet\bullet\bullet \mathrm{B}) - E(\mathrm{A}) - E(\mathrm{B}) \qquad (1)$$

where $E$(A•••B), $E$(A) and $E$(B) represent for the energies of supermolecule (A•••B), isolated A and B, respectively. When the value of $\Delta E$ is negative, the supermolecule is stabilized. The system in this study is composed of $Ti_{16}O_{32}(OH)_nH_n$ ($n$ = 0 and 1) slab, two $PhCH_2OH$ molecules, and one $O_2$ molecule. The reaction coordinates in the absence of $O_2$ were calculated in the singlet state, while those in the presence of $O_2$ were calculated in the singlet and/or

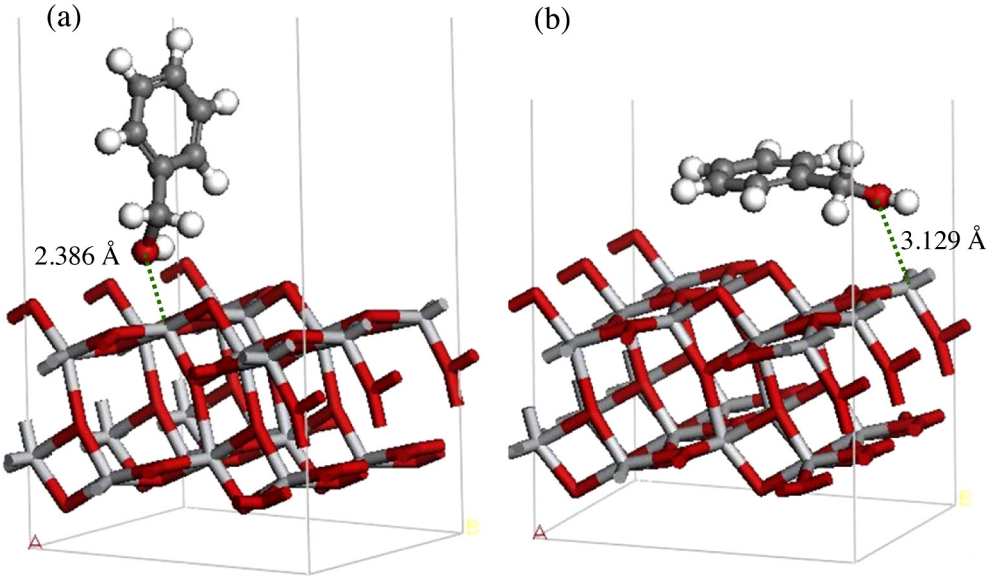


**Fig. 2.** Optimized structures by associative adsorption of benzyl alcohol ($Ti_{16}O_{32}$—$C_6H_5CH_2OH$) from (a) the vertical and (b) horizontal orientations.

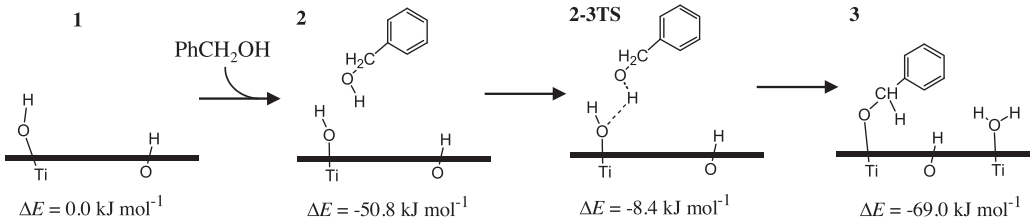


**Scheme 1.** Process for the formation of the alkoxide species by the interaction of benzyl alcohol with the [Ti]—OH on the $Ti_{16}O_{32}$(OH)H.

triplet states. And the lower $\Delta E$ in either the singlet or triplet state is shown in figures unless otherwise noted.

## 3. Results and discussion

### 3.1. Interactions of benzyl alcohol with $TiO_2$ surfaces

DFT calculations were carried out to clarify the possible electronic interactions of benzyl alcohol on the $TiO_2$ surface. The adsorption models of benzyl alcohol from vertical and horizontal orientations towards the $Ti_{16}O_{32}$ were optimized, and the results are shown in Fig. 2(a) and (b), respectively. It was calculated that the bond distance (2.386 Å) between the O of benzyl alcohol and the [Ti] site in (a) is shorter than that (3.129 Å) in (b). Furthermore, the adsorption energies (stabilization energies) in (a) and (b) were calculated to be −63.9 and −22.3 kJ mol$^{-1}$, respectively. This result suggests that (b) is less stable than (a), probably due to the repulsive interaction between the phenyl group and [O] of the $TiO_2$. Therefore, the adsorption model from the vertical orientation was adopted for further calculations.

The hydroxyl groups on the $TiO_2$ surface are considered to be one of the active species for an enhancement of the photocatalytic activity [31–36]. The presence of two types of OH groups involved on the $TiO_2$ surface were previously clarified: (1) one-fold-coordinated hydroxyl bonded to $Ti^{4+}$ ions (Ti—OH); and (2) two-fold-coordinated hydroxyl ions (>$OH^-$) resulting from protonation to the lattice oxygen ions (>$O^{2-}$).

Three types of interactions of benzyl alcohol with [Ti] of the $Ti_{16}O_{32}$ (i); [Ti]—OH (ii) and [O]—H (iii) of the $Ti_{16}O_{32}$(OH)H were modeled as shown in Fig. 3, and the results in the calculations are listed in Table 1. The stabilization energies were calculated to be −63.9 for (i), −50.8 for (ii) and −51.2 kJ mol$^{-1}$ for (iii). Moreover, the activation energy ($\Delta E_a$) for the dissociation of alcoholic O—H of the benzyl alcohol was calculated to be +72.6 for (i), +42.4 for (ii) and +74.9 kJ mol$^{-1}$ for (iii). The $\Delta E_a$ for (ii) was found to be much lower than that for (i) and (iii). The optimized structures and

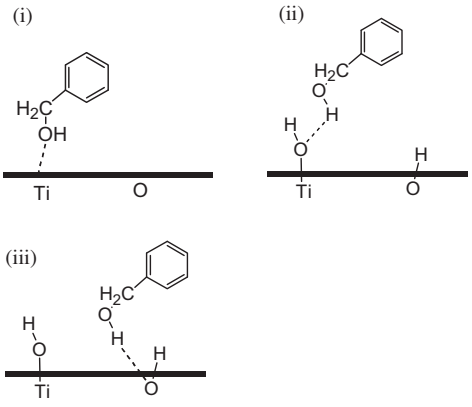


**Fig. 3.** Interactions of benzyl alcohol with (i) $Ti_{16}O_{32}$ and (ii) [Ti]—OH and (iii) [O]—H of the $Ti_{16}O_{32}$(OH)H.

**Table 1**
Activation energies to form alkoxides by the interaction of benzyl alcohol with different TiO2 surfaces corresponding to Fig. 3(i)–(iii).

| | (i) | (ii) | (iii) |
|---|---|---|---|
| | Energies/kJ mol$^{-1}$ | | |
| $\Delta E_{ads}$ [a] | −63.9 | −50.8 | −51.2 |
| $\Delta E_{TS}$ [b] | +8.7 | -8.4 | +23.7 |
| $\Delta E_a$ [c] | 72.6 | 42.4 | 74.9 |

[a] $\Delta E_{ads}$: stabilization energy by associative adsorption.
[b] $\Delta E_{TS}$: energy at the transitional state to abstract the alcoholic H.
[c] $\Delta E_a$: activation energies ($\Delta E_{TS} - \Delta E_{ads}$).

their electron density contour maps for (i) to (iii) are also shown in Figs. S1–S3, respectively. Small orbital mixing of benzyl alcohol with the $TiO_2$ surface in the band-gap region was observed in (i) and (iii), while large orbital mixing of the C—O region in benzyl alcohol with the O2p AOs of the VB was observed in (ii). These results suggests that the [Ti]—OH moiety plays a significant role in the strong hybridization with benzyl alcohol, leading to the formation of the alkoxide species.

### 3.2. Electronic structures of alkoxide species formed on the $TiO_2$ surface

Scheme 1 shows the process for the formation of the alkoxide species. The surface [Ti]—OH group (1) interacted with benzyl alcohol (2) can make a stable alkoxide species (3) through the transitional state of (2–3TS). Fig. 4 shows the optimized structures for (2), (2–3TS) and (3). The O—H bond in benzyl alcohol was elongated from 0.989 Å in (2) to 2.172 Å in (2–3TS), and completely dissociated to 4.093 Å in (3). Simultaneously, the O of the alkoxide species was bonded to the [Ti] site with 1.804 Å in (3).

Fig. 5 shows the projected density of states (PDOS) for the $Ti_{16}O_{32}$(OH)H [I] and configuration (3) [II a–c]. The zero of energy levels in Fig. 5[I] and [II a–c] indicate the highest occupied molecular orbitals (HOMOs). $TiO_2$ by itself exhibits a valence band mainly consisting of O2p AOs while the conduction band consisting of Ti 3d AOs with a band-gap of 3.05 eV, as shown in Fig. 5[I]. On the other hand, the PDOS for (3) exhibits two types of surface states at ca. −0.4 and 0 eV in Fig. 5[II-c], referred to as $\alpha$ and $\beta$, respectively, were observed in the band-gap region.

In order to verify the character of these surface states, Fig. 6 shows the electron density contour maps for (3). The orbital #211 at −0.783 eV forms the valence band maximum (VBM) of $TiO_2$, while #218 at +2.267 eV forms the conduction band minimum (CBM). The band-gap due to the intrinsic $TiO_2$ was estimated to be 3.05 eV, which is identical to that of $Ti_{16}O_{32}$(OH)H. One type of surface state ($\alpha$) consisting of the orbitals (#212–#215) originates with the alkoxide species hybridized with the O2p AOs in the VB of the $TiO_2$. In particular, the orbitals (#214 and #215) extend to the $PhCH_2O$—[Ti] bonding region, indicating that the O2p AOs in the alkoxide hybridizes with the Ti3d AOs by an electron-donating interaction. The energy gap between #215 and #218 was estimated to be 2.68 eV. The other surface state ($\beta$) consisting of the orbitals (#216 and #217) is localized within the phenyl ring.

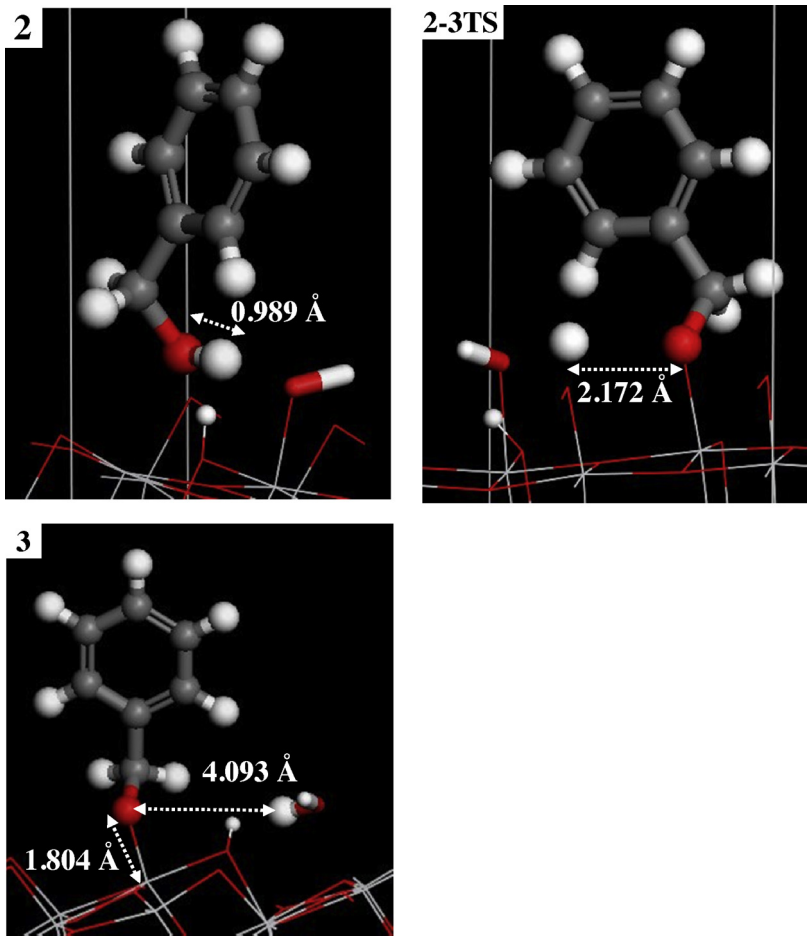


**Fig. 4.** Optimized structures for (2), (2–3TS) and (3).

The energy gap between #217 (HOMO) and #218 (CBM) was estimated to be 2.27 eV. These calculations clearly demonstrate that two types of surface states ($\alpha$ and $\beta$) are created in the band-gap region, as shown in Fig. S4. The surface states of $\alpha$ and $\beta$ are localized at 0.4 and 0.8 eV above the VBM, respectively. Here, if the photo-induced charge separation from the $\beta$ to CBM takes place, the holes left on the phenyl groups cannot significantly oxidize methylene groups judging from the energy levels of the orbitals (#216 and #217). Therefore, we suppose that the orbital mixing of the alkoxide species with the O2p AOs in the VBM is necessary for the visible-light induced reaction. Moreover, it was previously reported that $Nb_2O_5$ also exhibits visible-light responsive photocatalysis for the oxidation of alcohols. The visible-light response was assigned to the electronic excitation from the donor levels in the $Nb_2O_5$-alkoxide surface complex consisting of O2p AOs to the CB of the $Nb_2O_5$ by the DFT calculations [21,22]. We can thus assume that the origin for the visible-light response in the $TiO_2$ – alkoxide is mainly attributed to the excitation from the $\alpha$ level to the CBM, which can lead to the charge separation, i.e., hole in alkoxide and electron in Ti site.

### 3.3. *Possible reaction coordinates for the activation of benzyl alcohol*

Possible pathways for the activation of benzyl alcohol are shown in Scheme 2. Path 1 involves a dissociation process of the C—H bond by the surface [O]—H group without formation of the alkoxide species. First, [Ti]—OH (1) interacts with methylene H of benzyl alcohol (2″), which is activated through (2–3TS″) by +292.3 kJ mol$^{-1}$ (3.04 eV) to form (3″). Subsequently, (3″) was stabilized by replacement of $H_2O$ with $O_2$ (4″), followed by the reduction of $O_2$. Then, the alcoholic O—H bond was dissociated by assistance of superoxide anion (4–5TS″) to form benzaldehyde and hydro-peroxide (5″).

In path 2, the C—H bond in the alkoxide is dissociated by the surface [O]—H group. The formation of the alkoxide (3) has been demonstrated in Scheme 1. When the alkoxide (3) interacts with $O_2$ (4), it was less stabilized by +36.8 kJ mol$^{-1}$. However, it does not mean that $O_2$ adsorption was unstable, but does that the attractive interaction by $O_2$ is weaker than that by $H_2O$ since (4) is formed by replacement of $H_2O$ with $O_2$. The activation energy from (4) to (4–5TS′) was calculated to be +322 kJ mol$^{-1}$ (3.34 eV).

In path 3, the C—H bond in the alkoxide is dissociated by an assistance of $O_2$. In the structure of (4), the adjacent $O_2$ interacts with the methylene C—H (4–5TS). The structure of (4–5TS) was optimized in the singlet and triplet states, and the energies of (4–5TS) were calculated to be +189.9 and +226.5 kJ mol$^{-1}$, respectively. Therefore, the spin state changes from the triplet for (4) to the singlet for (4–5TS) in the course of the reaction. The methylene C—H bond is dissociated by assistance of $O_2$ through (4–5TS) with an activation energy of +153.1 kJ mol$^{-1}$ (1.59 eV), to form benzaldehyde and hydro-peroxide (OOH) species (5). It should be noted that the formation of the peroxide-like species on the $TiO_2$ surface is supported by experimental studies [10,18].

From these results, the energies for the abstraction of methylene H in the benzyl alcohol are required with 3.04 eV at 2–3TS″ in path 1, and 3.34 eV at 4–5TS′ in path 2. They can be only activated by the band-gap excitation of $TiO_2$ or higher, since the band-gap of the $TiO_2$ was calculated to be 3.05 eV as shown in Fig. 5. On

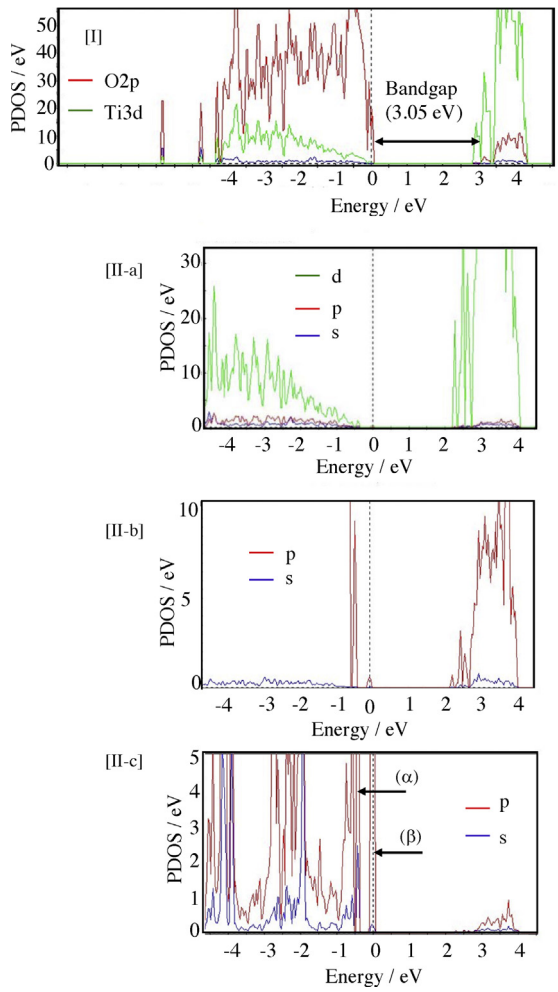


**Fig. 5.** Projected density of state (PDOS) for $Ti_{16}O_{32}(OH)H$ [I] and for (3) [II]: (a) Ti, (b) O and (c) benzyl alcohol.

**Table 2**
Characteristic bond distances in the methylene C—H dissociation.

| | 4 | 4–5TS | 5 |
|---|---|---|---|
| | Bond distance/Å | | |
| [a]C—H | 1.102 | 1.284 | 3.458 |
| [b]O—O | 1.239 | 1.307 | 1.446 |
| [c]C—O | 1.440 | 1.345 | 1.244 |
| [d]Ti—O(—$H_2$C—ph) | 1.824 | 2.056 | 2.485 |

the other hand, the activation energy of 1.59 eV at 4–5TS in path 1 is less than the others, and it can be surmounted by visible-light irradiation. Therefore, path 3 was confirmed to be the most energetically favorable route for the abstraction of methylene H from benzyl alcohol among paths 1–3.

Fig. 7 shows the characteristic electron-density contour maps of the HOMO (#219) and next-HOMO (#218) in the singlet state for (4–5TS). The #219 exhibits the localized $\pi^*$ orbital in the $O_2$ region, whereas the #218 exhibits a hybridized orbitals of the alkoxide species with the hydro-peroxy species. Fig. 8 shows the optimized structures for the (4), (4–5TS) and (5), and their corresponding bond distances are shown in Table 2. It was observed that the bond distance for C—H was elongated from 1.102 Å (4) to 3.458 Å (5), and that for O—O was from 1.239 Å (4) to 1.446 Å (5). These results suggest that the electron transfer takes place from the alkoxide to the $\pi^*$ orbitals in $O_2$. It was experimentally confirmed that the presence of $O_2$ atmosphere is essential for the oxidation of the benzyl alcohol under visible-light irradiation. Taking the results of calculations into considerations, the role of photo-induced hole and electron formed in the alkoxide ([Ti]—O—$CH_2$—ph) species under visible-light irradiation is proposed as shown in Fig. 9. The hole participates in the oxidation of the alkoxide species, while the electron participates in the reduction of $O_2$ to form superoxide anion ($O_2^-$). Subsequently, the $O_2^-$ assists the dissociation of the methylene C—H bond to form benzaldehyde and hydro-peroxide species. It was also observed that the bond distance for C—O in the alkoxide decreased from 1.440 Å (4) to 1.244 Å (5), and that for Ti—O(—$H_2$C—ph) increased from 1.824 Å (4) to 2.485 Å (5), indicating that the carbonyl species is significantly formed and it leaves from the $TiO_2$ surface. The configuration (5) does not exhibit orbital mixing between the $TiO_2$ surface and benzaldehyde produced (see Fig. S5).

In order to complete the reaction, another benzyl alcohol molecule should be oxidized stepwise. One of the possible reaction paths for the oxidation of the benzyl alcohol by the hydro-peroxide (OOH) species is demonstrated in Scheme 3 and their optimized structures are shown in Fig. S6. When the hydro-peroxide species interacts with benzyl alcohol (6), the alcoholic H atom in benzyl alcohol is abstracted through (6–7TS) to form the alkoxide and hydrogen peroxide (7). The activation energy (+16.2 kJ $mol^{-1}$) from (6) to (6–7TS) can be easily surmounted by thermal reaction while the dissociation of the methylene C—H bond through (7–8TS) produces benzaldehyde accompanied by the re-generation of the Ti—OH group (8) and $H_2O$. The reaction through (7)–(7–8TS) requires a relatively high activation energy of +203.5 kJ·$mol^{-1}$ (2.11 eV). The electron density contour plots of configuration (7) exhibits the donor levels (#215, #217) attributed to the orbital

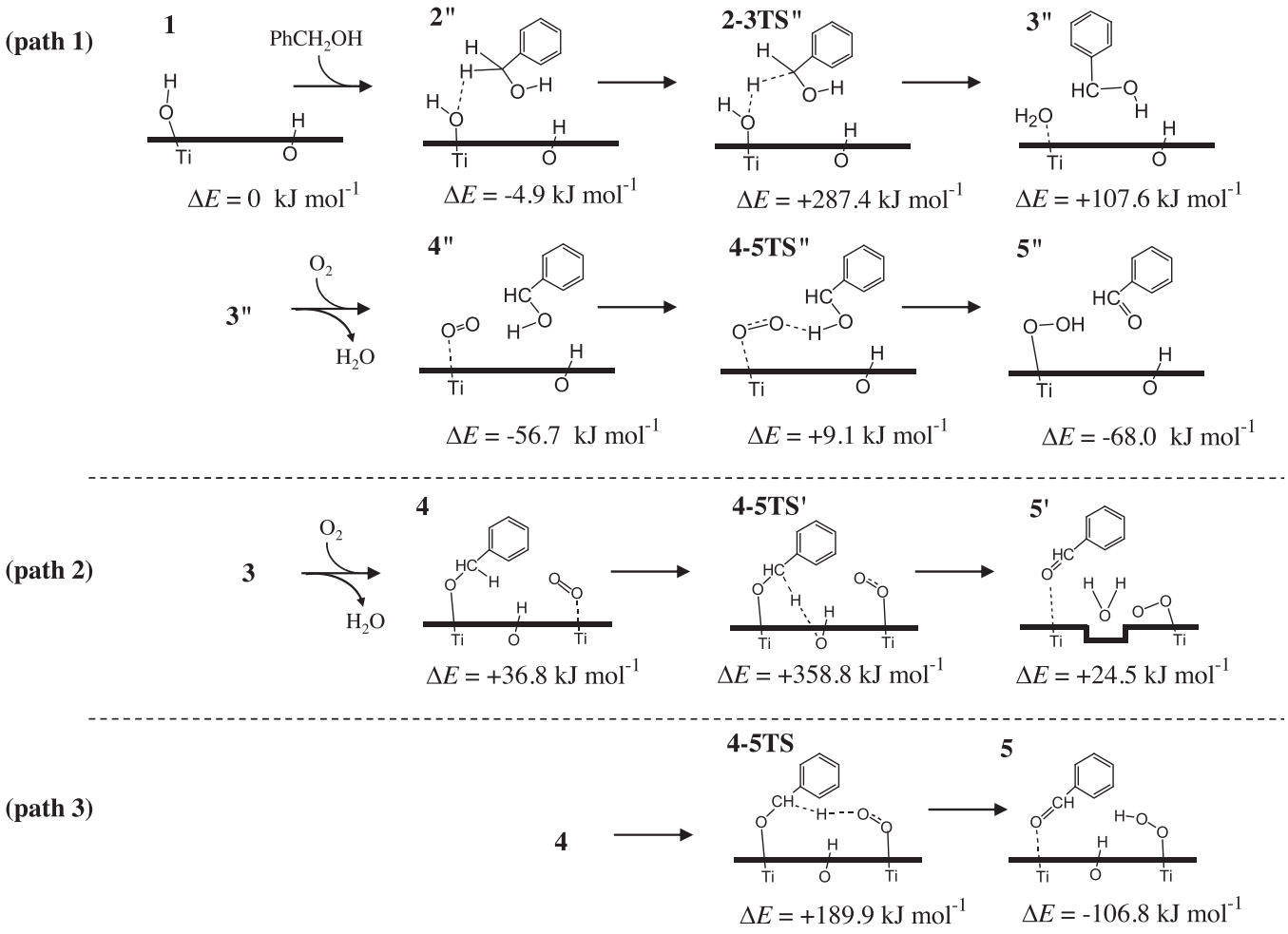


**Scheme 2.** Possible reaction coordinates for the C—H dissociation by [Ti]—OH (path 1), [O]—H (path 2) and $O_2$ (path 3).

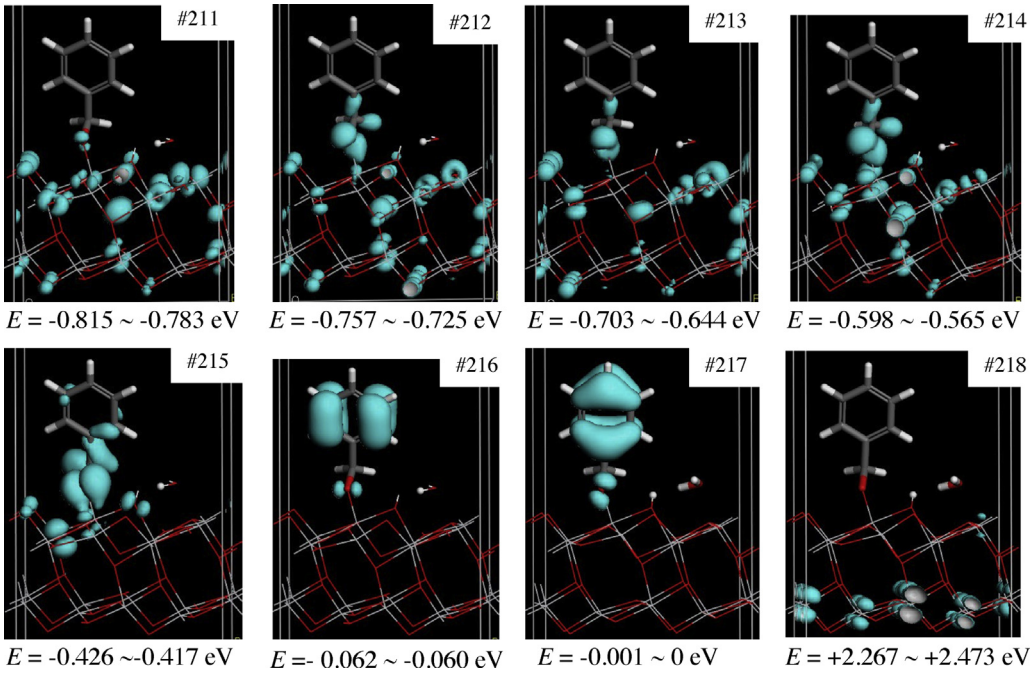


**Fig. 6.** Electron density contour maps for (3).

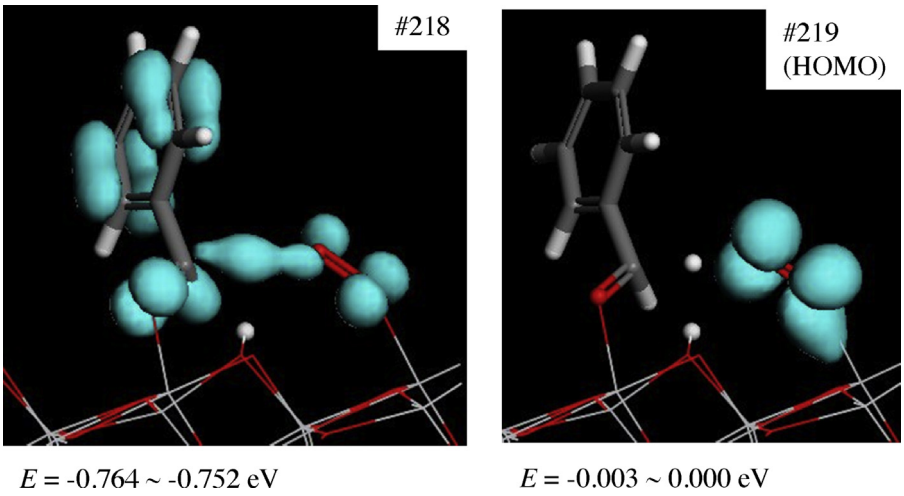


**Fig. 7.** Orbital electron density contour maps (HOMO and next HOMO) for (4–5TS) in the singlet state.

mixing of the alkoxide species with the O2p AOs in the VBM as shown in Fig. S7. The electronic transition from the donor levels to the CBM of the $TiO_2$ can be possibly induced by visible-light, leading to dissociation of the C—H bond. Overall reaction coordinates in path 3 are shown in Fig. 10. As shown in Fig. 10, the relatively high activation energies: +153.1 kJ $mol^{-1}$ (1.59 eV) from (4) to (4–5TS) and +203.5 kJ·$mol^{-1}$ (2.11 eV) from (7) to (7–8TS) are required for the dissociation process of the methylene C—H of the alkoxide species. These activation energies are lower energies than the $TiO_2$ band-gap transition (3.05 eV), suggesting that both TSs

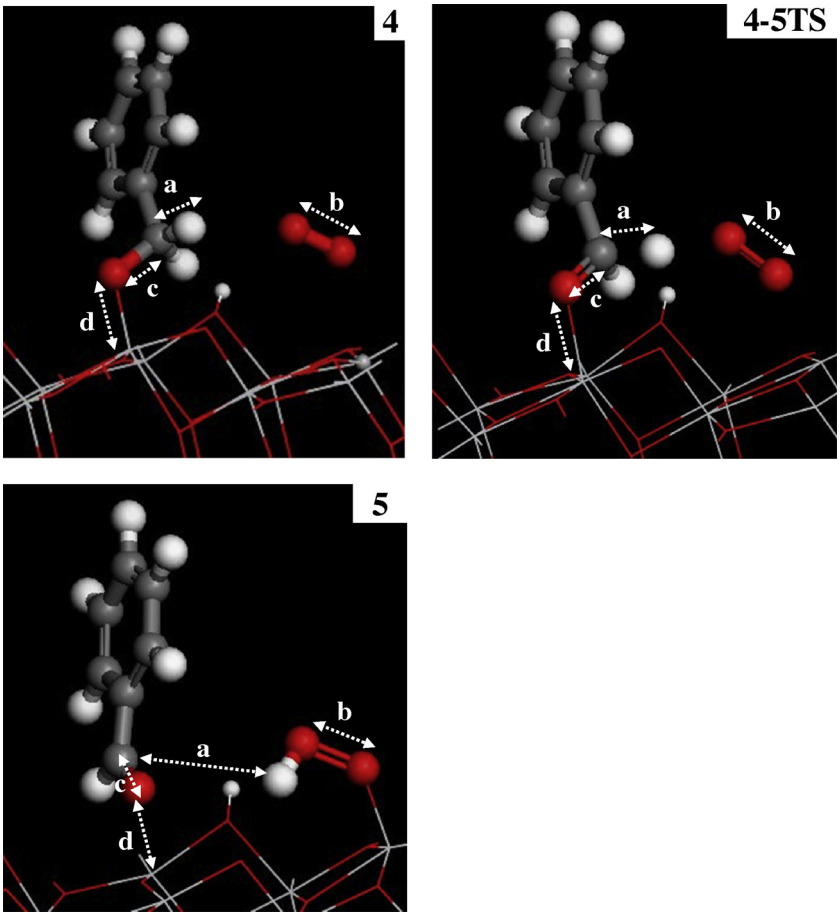


**Fig. 8.** Optimized structures for (4), (4–5TS) and (5).

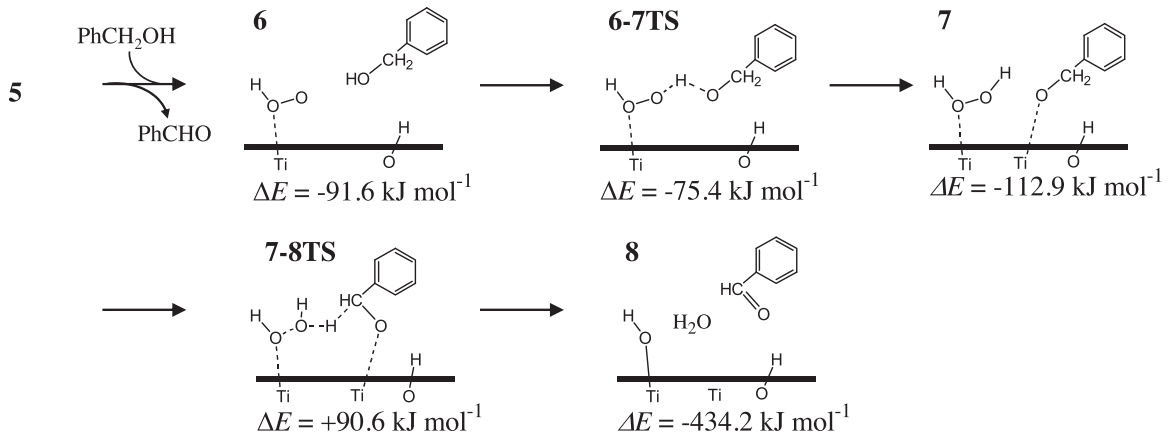


**Scheme 3.** Reaction coordinates for the oxidation of benzyl alcohol by the hydro-peroxide species formed on the $TiO_2$ surface.

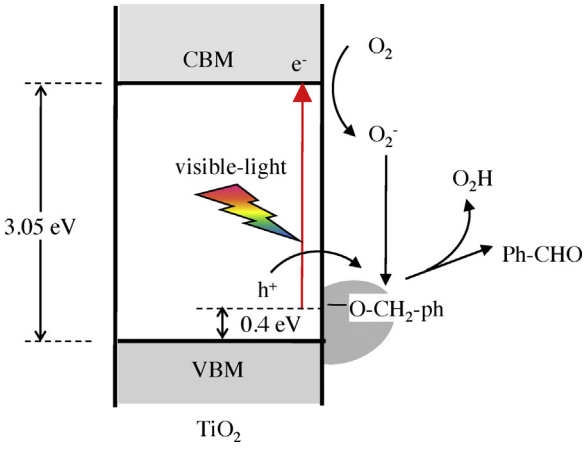


**Fig. 9.** Role of electron transfers under visible-light irradiation and initial reaction for the oxidation of benzyl alcohol.

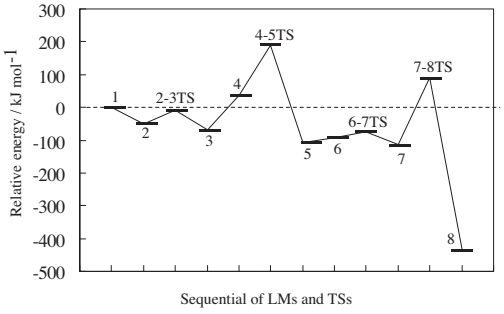


**Fig. 10.** Overall reaction coordinates for the sequential LMs and TSs in (path 3).

should be surmounted by the visible light irradiation. That is, irradiations of two photons are required for the oxidation of two benzyl alcohol into two benzaldehydes through four electron-transfers.

## 4. Conclusions

The reaction mechanism for the selective catalytic oxidation of benzyl alcohol into benzaldehyde was investigated by DFT calculations. It was found that the interactions of benzyl alcohol with the [Ti]—OH group of the $TiO_2$ surface form alkoxide species. The origin of the visible-light response was confirmed to be attributed mainly to the electronic transition from the donor levels created by the alkoxide species to the CBM of the $TiO_2$. Furthermore, reaction coordinates in the overall catalytic reaction of benzyl alcohol into benzaldehyde on the $TiO_2$ surface were demonstrated, and the role of the visible-light irradiation was clearly shown. This study can thus contribute to a deeper understanding of the electronic structures for the catalytic oxidation of alcohols as well as the role of the visible-light irradiation on this catalytic system.

## Acknowledgements

The authors are grateful to Prof. Jie Fan and Dr. Renhong Li of Zhejiang University (China) for their valuable discussions.

## Appendix A. Supplementary data

Supplementary data associated with this article can be found, in the online version, at http://dx.doi.org/10.1016/j.apcatb.2015.01.035.

## References

[1] G.J. Brink, I.W.C.E. Arends, R.A. Sheldon, Science 287 (2000) 1636.
[2] T. Mallat, A. Baiker, Chem. Rev. 104 (2004) 3037.
[3] M. Nechab, C. Einhorn, J. Einhorn, Chem. Commun. 13 (2004) 1500.
[4] M.A. Fox, M.T. Dulay, Chem. Rev. 93 (1993) 341.
[5] Y. Shiraishi, T. Hirai, J. Photochem. Photobiol. C: Photochem. Rev. 9 (2008) 157.
[6] G. Palmisano, E. García-López, G. Marcì, V. Loddo, S. Yurdakal, V. Augugliaro, L. Palmisano, Chem. Commun. 46 (2010) 7074.
[7] X. Lang, X. Chen, J. Zhao, Chem. Soc. Rev. 43 (2014) 473.
[8] S. Yurdakal, G. Palmisano, V. Loddo, V. Augugliaro, L. Palmisano, J. Am. Chem. Soc. 130 (2008) 1568.
[9] R. Li, H. Kobayashi, J. Guo, J. Fan, J. Phys. Chem. C 115 (2011) 23408.
[10] Q. Wang, M. Zhang, C. Chen, W. Ma, J. Zhao, Angew. Chem. Int. Ed. 122 (2010) 8148.
[11] S. Higashimoto, N. Kitao, N. Yoshida, T. Sakura, M. Azuma, H. Ohue, Y. Sakata, J. Catal. 266 (2009) 279.
[12] S. Higashimoto, K. Okada, T. Morisugi, M. Azuma, H. Ohue, T.-H. Kim, M. Matsuoka, M. Anpo, Top. Catal. 53 (2010) 578.
[13] S. Higashimoto, N. Suetsugu, M. Azuma, H. Ohue, Y. Sakata, J. Catal. 274 (2010) 76.
[14] S. Higashimoto, K. Okada, M. Azuma, H. Ohue, T. Terai, Y. Sakata, RSC Adv. 2 (2012) 669.
[15] M. Zhang, C. Chen, W. Ma, J. Zhao, Angew. Chem. Int. Ed. 47 (2008) 9730.
[16] S. Naya, A. Inoue, H. Tada, J. Am. Chem. Soc. 132 (2010) 6292.
[17] A. Tanaka, K. Hashimoto, H. Kominami, J. Am. Chem. Soc. 134 (2012) 14526.
[18] S. Higashimoto, R. Shirai, Y. Osano, M. Azuma, H. Ohue, Y. Sakata, H. Kobayashi, J. Catal. 311 (2014) 137.
[19] S. Kitano, A. Tanaka, K. Hashimoto, H. Kominami, Phys. Chem. Chem. Phys. 16 (2014) 12554.
[20] Z. Zhang, Z. Luo, Z. Yang, S. Zhang, Y. Zhang, Y. Zhou, X. Wang, X. Fu, RSC Adv. 3 (2013) 7215.
[21] T. Shishido, T. Miyatake, K. Teramura, Y. Hitomi, H. Yamashita, T. Tanaka, J. Phys. Chem. C 113 (2009) 18713.
[22] S. Furukawa, Y. Ohno, T. Shishido, K. Teramura, T. Tanaka, ChemPhysChem 12 (2011) 2823.

[23] F. Su, S.C. Mathew, G. Lipner, X. Fu, M. Antonietti, S. Blechert, X. Wang, J. Am. Chem. Soc. 132 (2010) 16299.
[24] A. Vittadini, M. Casarin, A. Selloni, Theor. Chem. Acc. 117 (2007) 663.
[25] C.B. Mendive, T. Bredow, A. Feldhoff, M.A. Blesa, D. Bahnemann, Phys. Chem. Chem. Phys. 11 (2009) 1794.
[26] M.C. Payne, M.P. Teter, D.C. Allan, T.A. Arias, J.D. Johnnopoulos, Rev. Mod. Phys. 64 (1992) 1045.
[27] V. Milman, B. Winkler, J.A. White, C.J. Pickard, M.C. Payne, E.V. Akhmatskaya, R.H. Nobes, Int. J. Quantum Chem. 77 (2000) 895.
[28] P. Perdew, K. Burke, M. Ernzerhof, Phys. Rev. Lett. 77 (1996) 3865.
[29] P. Perdew, K. Burke, M. Ernzerhof, Errata, Phys. Rev. Lett. 78 (1997) 1396.
[30] D. Vanderbilt, Phys. Rev. B 41 (1990) 7892.
[31] C. Deiana, E. Fois, S. Coluccia, G. Martra, J. Phys. Chem. C 114 (2010) 21531.
[32] A.Y. Nosaka, J. Nishino, T. Fujiwara, T. Ikegami, H. Yagi, H. Akutsu, Y. Nosaka, J. Phys. Chem. B 110 (2006) 8380.
[33] G.D. Parfitt, Prog. Surf. Membr. Sci. 11 (1976) 181.
[34] J.F. Montoya, I. Ivanova, R. Dillert, D.W. Bahnemann, P. Salvador, J. Peral, J. Phys. Chem. Lett. 4 (2013) 1415.
[35] L.E. Walle, A. Borg, E.M.J. Johansson, S. Plogmaker, H. Rensmo, P. Uvdal, A. Sandell, J. Phys. Chem. C 115 (2011) 9545.
[36] Y. Li, Y. Gao, Phys. Rev. Lett. 112 (2014) 206101.